

A Summary of Spacecraft Charging Results

P.F. Mizera*

The Aerospace Corporation, El Segundo, California

The satellite surface potential monitor, flown on the USAF P78-2 satellite, measured spacecraft differential charging in the near geosynchronous orbit. Negative charging, greater than 100 V relative to spacecraft ground, occurred more than 10% of the time between 20 and 09 h local time during magnetically disturbed conditions. In particular, Kapton samples charged greater than -100 V over 50% of the time in the 05 to 06 h local time interval when $K_p > 2+$. Charging levels greater than -1000 V occurred in the premidnight sector a few percent of the time. The electrical conductivity of Kapton increased after exposure to sunlight to such an extent that its surface charging decreased by orders of magnitude after one year in space. Conversely the quiescent potential level of Teflon increased with time. Optical solar reflector mirrors charged infrequently and to very small levels. Quartz fabric reached potentials even greater than Kapton during charging events, contrary to predictions.

Introduction

IN the mid-1970's a study to explain geosynchronous satellite anomalies was initiated under a program called Spacecraft Charging at High Altitudes (SCATHA). For an in-depth discussion of spacecraft charging the reader is referred to Refs. 1 and 2. An integral part of the SCATHA program was the flight of the USAF P78-2 satellite. The experiments aboard were designed to measure the environment near geosynchronous altitude and the effects of the environment on spacecraft materials.³

The P78-2 satellite is a spin stabilized, cylindrically shaped structure approximately 1.75 m in both length and diameter which was placed into a near geosynchronous orbit late in January 1979. Two solar cell arrays, separated by a conducting bellyband, completely encircled the vehicle. The top and bottom contained the apogee insertion motor cavity and the communications antenna, respectively. Additional information about the satellite and the payloads can be found in Refs. 4 and 5.

Voltages and currents from typical spacecraft materials were obtained from the satellite surface potential monitor (SSPM) experiment. The SSPM-1 and SSPM-2 instruments were mounted near the bellyband 180 deg apart, and the SSPM-3 was mounted on the bottom of the vehicle. For the first time, differential spacecraft charging was studied in space under a variety of orbital and geophysical conditions.

In addition to individual charging events, long-term analyses were made to determine the statistical nature of the occurrence of charging and the stability of material properties. Long-term (7-10 years) stability to the vacuum, solar ultraviolet (uv) flux, and charged particle environment are important requirements for future space programs.⁶ The SSPM results, correlated with measurements of the environment and measured discharge pulses, should make a significant contribution to future space programs.

Experiment Background

Nine spacecraft materials were mounted over electrostatic field meters to obtain the back surface voltages during charging events. Each sample was mounted at a fixed position from the sensor to allow a voltage measurement. The dc current passing through a sample and the capacitively coupled

current were collected on a copper clad circuit board and routed to a high impedance amplifier circuit which digitized both positive and negative currents. Table 1 lists the materials flown on the SSPM experiment. Details of the measurement techniques can be found in Refs. 4, 7, and 8.

In order for a material to charge negatively in the space environment, the electron current above the second crossover energy must be greater than the discharging or neutralizing currents.⁹ (The second crossover energy is where the secondary electron coefficient becomes less than unity.) That is,

$$I_e^2 > I_e^1 + I_{pe} + I_{se} + I_i \quad (1)$$

where I_e^2 is the electron current above the second crossover (negative); I_e^1 is the electron current below the second crossover (positive); I_{pe} is the electron current due to photoelectrons (positive); I_{se} is the electron current due to secondary electrons (positive); and I_i is the ion current (positive).

Except during spring and fall eclipse seasons, the P78-2 satellite is in sunlight and the solar uv flux is usually sufficiently intense to keep the sunlit materials near vehicle ground potential. Potentials can never get very positive because of the low-energy electrons that usually surround the spacecraft.

The SSPM-1 and SSPM-2 instruments were mounted near the bellyband of the spacecraft and rotated into and out of sunlight every 30 s except during the eclipse seasons. In addition to Kapton, there were two optical solar reflector (OSR) samples mounted on the SSPM-1. One was coated with indium oxide and grounded to the vehicle frame. The SSPM-2 instrument contained a large single Kapton sample from which the standard back surface potential measurement was obtained and in addition, a 1-in. hole was centered over one electrostatic field meter to allow a measurement of the front surface potential. The potential of a gold plated reference band which surrounded the vehicle was measured by routing the signal to the SSPM-2 instrument by means of a coaxial cable. This signal provided an absolute reference to the SSPM by means of solar uv illuminating approximately 50% of its area except during eclipse periods.

The SSPM-3 samples were normally in the vehicle shadow on one end of the spacecraft. The quartz fabric sample was mounted on Teflon and the gold flashed Kapton was grounded to the vehicle frame.

Results

Two charging events, one in sunlight and one in eclipse, were described previously.⁸ Figure 1 is a reproduction of one

Presented as Paper 82-0268 at the AIAA 20th Aerospace Sciences Meeting, Orlando, Fla., Jan. 11-14, 1982; submitted Jan. 20, 1982; revision received June 24, 1983. Copyright © American Institute of Aeronautics and Astronautics, Inc., 1982. All rights reserved.

*Member of the Technical Staff, Space Sciences Laboratory. Associate Fellow AIAA.

of those events to illustrate the levels reached by different dielectric materials. The top two curves are 1-s samples of the SSPM-1 and SSPM-2 Kapton voltages. The down-pointing arrows indicate when each sample entered sunlight, and the up-pointing arrows show when the sample entered the shadow of the spacecraft. The SSPM-3 samples, shown at the bottom of Fig. 1, are in the shadow of the spacecraft. These latter samples are mounted with their surface normals parallel to the spin axis of the spacecraft. Note that during this brief 130-s time period, there are striking differences between the charging profiles of the bellyband and the SSPM-3 Kapton samples. As Ref. 8 showed, the bellyband Kaptons began to charge some 17 min before the SSPM-3 samples. Equation (1) shows that the charging current is a sensitive function of the charged particle environment and the location of sample may be important.

Figure 2 compares the surface voltage of Kapton to the incident current obtained by integrating the electron distribution over energies from 5 to 80 keV. The electron measurements were obtained from a spectrometer flown on the P78-2 satellite.¹⁰ The data were averaged over a satellite rotation period of approximately 60 s. During this time, the Kapton sample was charging only during the time it was in the shadow of the spacecraft. Therefore the voltage levels reached

in each sample period were not the final equilibrium values.⁸ Nevertheless, if one examines Eq. (1), I_e^2 is the dominant contributor to the charging observed on April 21, 1979 and is a sensitive indicator of the magnitude of the charging potential. Once the second crossover (~ 1 keV) of Kapton is exceeded, the current from the energetic electrons plays the dominant role in spacecraft charging, especially in shadow.

A survey of such individual charging events was done for days 38 to 273, 1979. The survey was primarily intended to catalog levels of differential charging and accumulate these data as a function of geophysical, orbital, and other parameters. A preliminary summary was presented at the 3rd Spacecraft Charging Conference held in November 1980.¹¹

Table 1 SSPM samples

Unit	Material
1	Kapton
	OSRs
	Gold on magnesium
2	Kapton
	Reference band
3	Kapton
	Teflon
	Quartz fabric
	Gold on Kapton

Table 2 64-s intervals in the SSPM survey

MLT	$L \leq 6.6 R_e$		$L > 6.6 R_e$	
	$K_p \leq 2+$	$K_p > 2+$	$K_p \leq 2+$	$K_p > 2+$
0-3	1,706	1,780	21,114	19,898
3-6	4,131	3,751	17,454	17,567
6-9	8,607	6,218	10,934	12,944
9-12	12,022	10,224	5,660	5,954
12-15	14,116	11,939	2,048	3,241
15-18	10,725	9,712	6,964	6,138
18-21	6,839	6,520	13,946	11,492
21-24	3,055	3,528	18,958	17,265

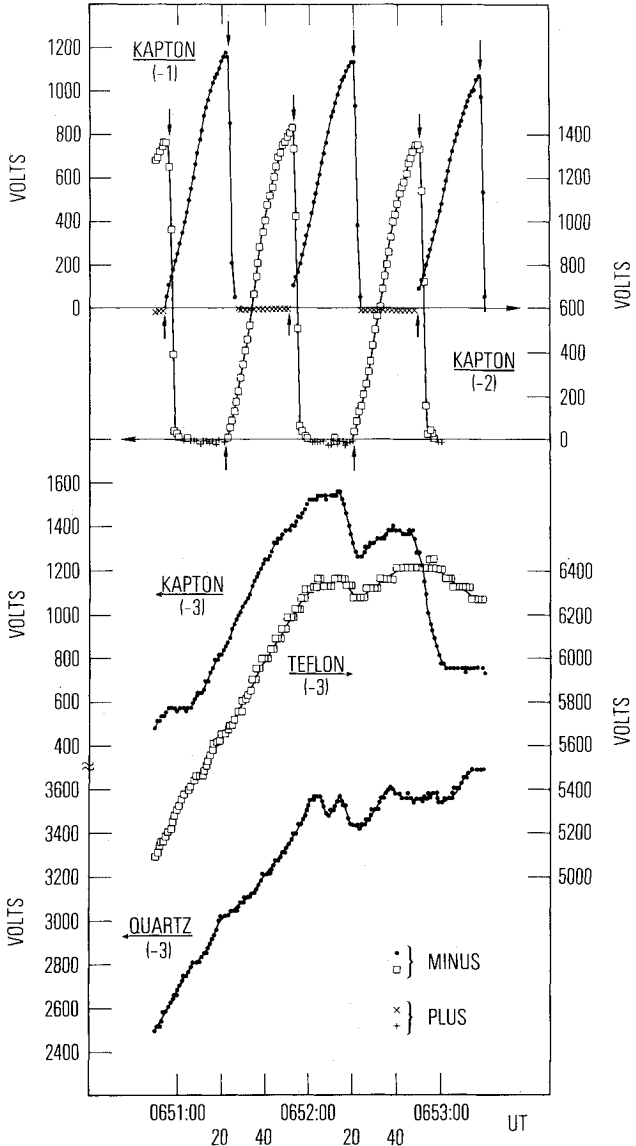


Fig. 1 SSPM voltages for the April 24, 1979 daylight charging event. The data are plotted vs universal time.

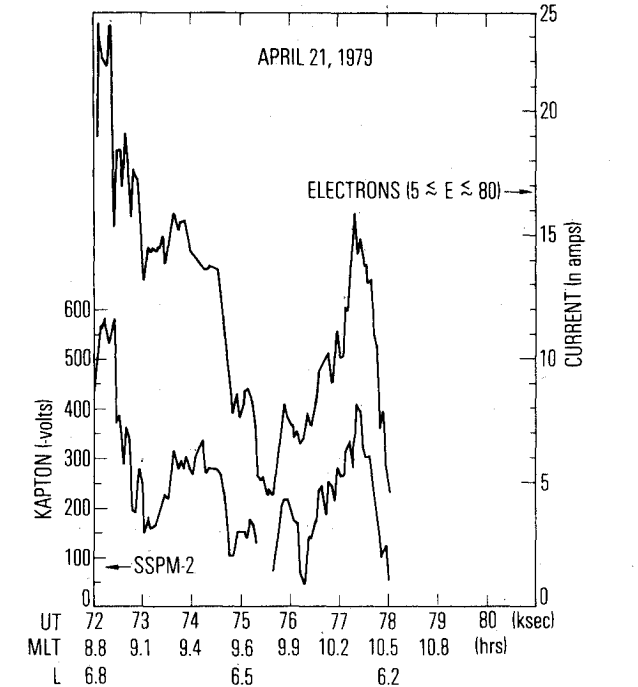


Fig. 2 Kapton surface potential and calculated current to the sample using the electron spectrum from 5 to 80 keV. (A current of 25 nA is equivalent to ~ 30 pA/cm².)

Table 2 shows the number of 64-s time intervals in the survey as a function of magnetic local time (MLT) 3-h intervals, altitude above and below geosynchronous ($\sim 36,000$ km), and magnetic activity defined by the standard global 3-h index K_p . Geosynchronous altitude is also defined by the L -shell parameter (equal to $6.6 R_e$). This parameter describes charged particle motion in the Earth's magnetic field. L is the number of Earth radii (R_e) to an object in space (at the magnetic equator) from the center of the Earth. Off the equator, L scales as $R_e \cos^{-2} \lambda_m$, where λ_m is the magnetic latitude of the Earth.

There are regions in this three-dimensional space matrix where the coverage is less than desired. For example, the satellite spent only approximately 28.2 h out of the 7½ months at low altitudes during quiet magnetic conditions in the postmidnight sector. Conversely, over 371 h were spent above geosynchronous altitudes during quiet times in the postmidnight sector. Nevertheless, all sectors were covered with sufficient statistical accuracy to estimate where differential charging was likely to occur. It should also be pointed out that the data samples are not independent of each other. That is, a given time period was divided into 64 s intervals. If a charging event was occurring, then the probability that consecutive samples would show charging was high and vice versa.

Figure 3 shows the probabilities of charging for the two bellyband Kapton samples. High- and low-altitude data are plotted as a function of 3-h local time intervals during disturbed conditions. $K_p = 2_+$ marks the transition from magnetically quiet times to disturbed times. Both Kapton samples behaved in a similar fashion with slightly higher probabilities for Kapton-2. Kapton-2 was a factor of 5 larger in area than Kapton-1 or Kapton-3. The SSPM data clearly show that differential charging is most likely to occur 6-9 h past local midnight and is at least a factor of 2 more probable above geosynchronous altitude than below.

When we examine the data acquired during quiet magnetic conditions, the charging drops dramatically, as shown in Fig. 4. In fact, charging is almost nonexistent below geosynchronous orbit during quiet times.

Figure 5 shows the charging probabilities for the gold-plated magnesium conductor and the ungrounded optical solar reflector samples mounted on the SSPM-1. Gold and OSRs have much lower charging probabilities than Kapton. This is primarily due to the large secondary electron yields for gold and OSRs and the higher-energy second crossover in the secondary electron yield function for these materials. The OSRs reached levels greater than -100 V during only a few percent of the charging events.

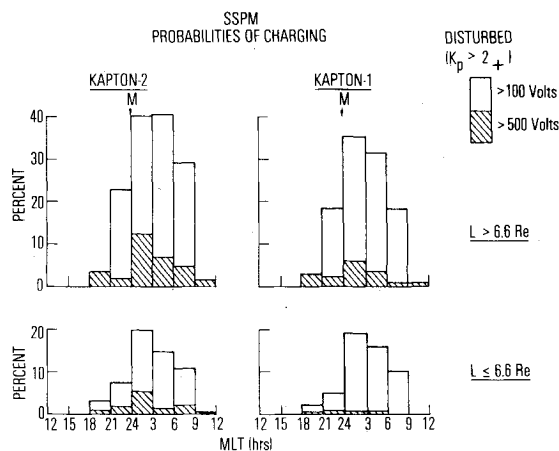


Fig. 3 Probabilities of charging > -100 V and > -500 V for the two bellyband Kapton samples during disturbed magnetic conditions (M denotes local midnight).

The overall trends of the gold conductor charging probabilities are similar enough to those of Kapton and presumably of other dielectrics to infer a typical charging profile. Therefore we have averaged data from the two bellyband Kapton samples to make a "typical" charging probability profile for the near geosynchronous orbit as a function of local time. Figure 6 shows this differential charging profile for what we call a typical satellite material in a geosynchronous orbit during disturbed magnetic conditions. The absolute percentages are dependent on the materials used and details of the measurement technique, but the trends shown in Fig. 6 should be representative of spacecraft

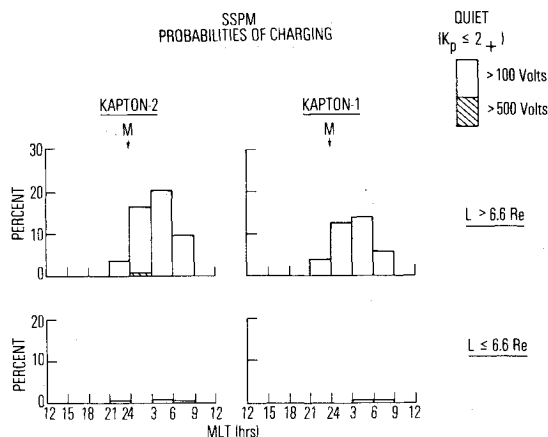


Fig. 4 Same as Fig. 3, but for quiet magnetic conditions.

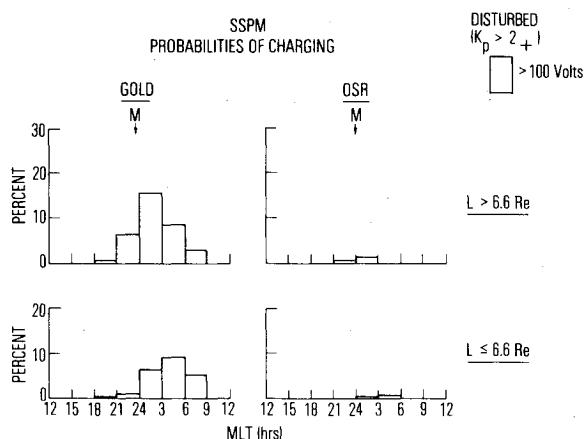


Fig. 5 Gold and OSR charging probabilities during disturbed magnetic conditions.

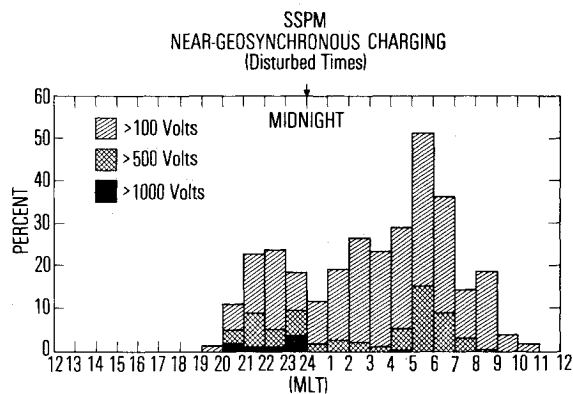


Fig. 6 Charging probabilities of Kapton for the geosynchronous orbit during disturbed magnetic conditions.

material charging in shadow. The majority of charging at low voltage levels occurs near dawn local time but higher levels of voltages occur before midnight.

Figure 7 shows the complete SSPM survey results for the bellyband Kapton-2 sample. The light gray patches represent regions where the coverage is less than 90 min in time. Both the 10% and 50% charging probabilities of greater than -100 V are shown in Fig. 7. Outside of the 10% contour, we do not expect differential spacecraft charging to be important. The 10% level of charging greater than -1000 V is also shown and is predominantly a premidnight phenomenon at low altitudes and moves to higher altitudes near midnight.

It is interesting to compare the local time spacecraft charging distribution from the ATS-6 satellite¹² with the charging distribution shown in Fig. 7. The premidnight boundaries of charging are within an hour of each other, and the dawn boundaries (although more complicated) also show good agreement. It is encouraging that two different data sets using different experimental techniques at two different times could provide this kind of agreement.

Figure 1 showed charging data a few months after launch. A second event, which occurred on June 10, 1980, is shown in Fig. 8. The format is similar to Fig. 1, but the data are averaged over a longer time interval. The top two curves represent the bellyband Kapton voltages averaged over 30 s in the sun and in the shadow. Note that the bottom three sample voltages from the SSPM-32 instrument are higher than those observed on April 24, 1979. However, in the earlier charging event, the bellyband Kapton samples reached values of approximately -1200 and -1400 V, whereas some 14 months later, voltages of only a few volts were recorded. Thus after exposure to the space environment of less than 18 months, two of the three Kapton samples became poor insulators.

Changes in the bellyband Kapton samples are illustrated in Figs. 9a and 9b. For a given 24-h period, the maximum voltage from Kapton was divided by the maximum voltage from the gold conductor sample. These ratios were arbitrarily

normalized and plotted on a semilogarithmic time scale. A straight line fit to the data shows decay slopes of 0.011 and 0.012 days⁻¹, respectively. Using gold as a reference voltage, the changes in the Kapton voltages should mimic the changes in the Kapton resistivity with time. Based on this analysis, Kapton loses its insulating properties when exposed to solar uv over a period of time. The drop in resistivity had a time constant of approximately 3 months when Kapton was solar illuminated with a 50% duty cycle.

Strictly speaking, the ratio of Kapton voltage to the gold voltage is not necessarily the same as the measurement of the bulk resistivity. In order to properly measure the resistivity, equilibrium conditions must be established. Most of the data in Fig. 9 were taken in daylight when the sample was in the spacecraft shadow for only 30 s and equilibrium cannot take place in so short a time period.

Figure 10 shows the voltage levels of the silvered Teflon sample with time. Each point represents the voltage recorded when the P78-2 satellite was near local noon. As Figs. 3-5 showed, there is no surface charging in the local noontime sector. Two effects are evident in Fig. 10: 1) There is a long-term increase in the voltage level of Teflon, and 2) there are short-term variations that appear to increase with time. The short-term variations probably result from two distinct ef-

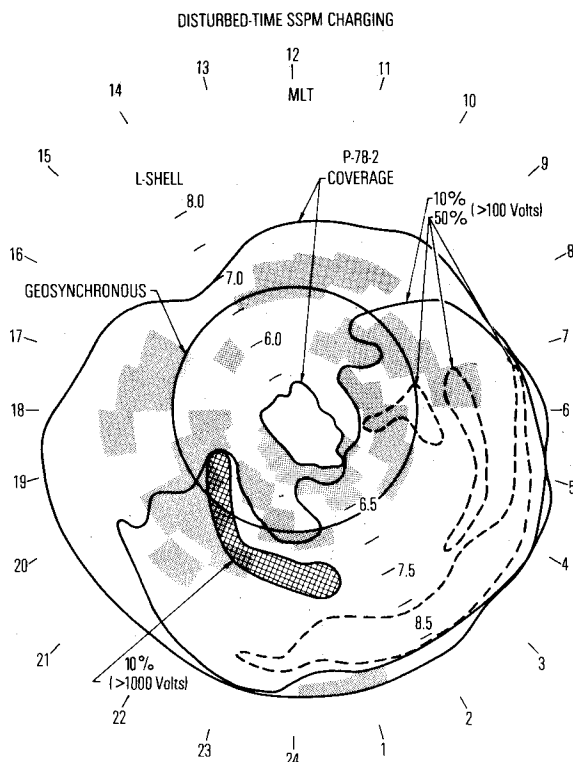


Fig. 7 Polar plot of the $>10\%$ and $>50\%$ charging probability of Kapton > -100 V as a function of L -shell and local time. Also shown is the $>10\%$ probability > -1000 V. The shaded areas represent poor satellite coverage.

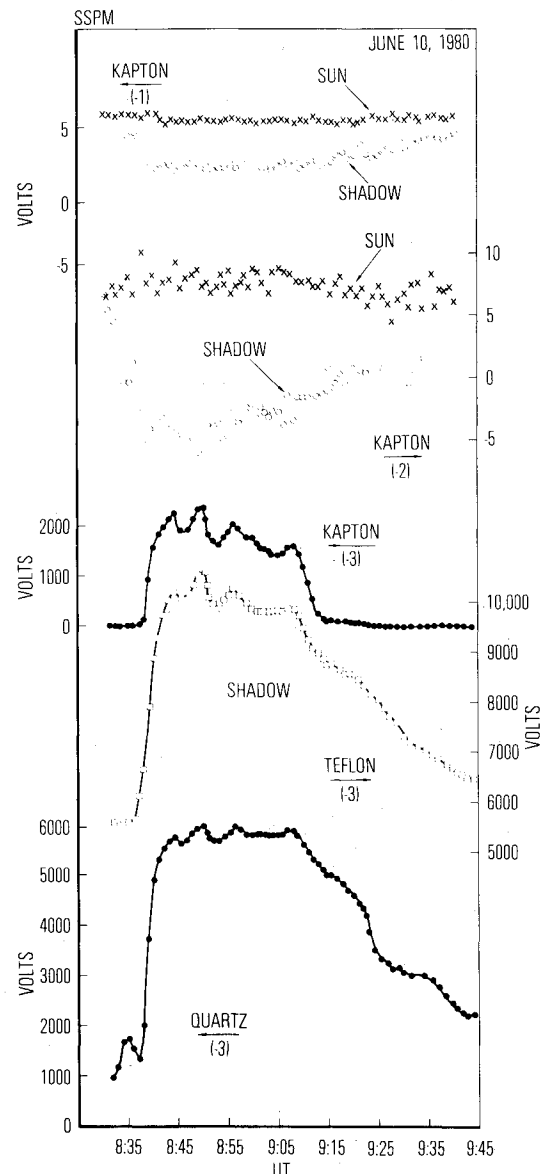


Fig. 8 Same format at Fig. 1, but for a charging event on June 10, 1980.

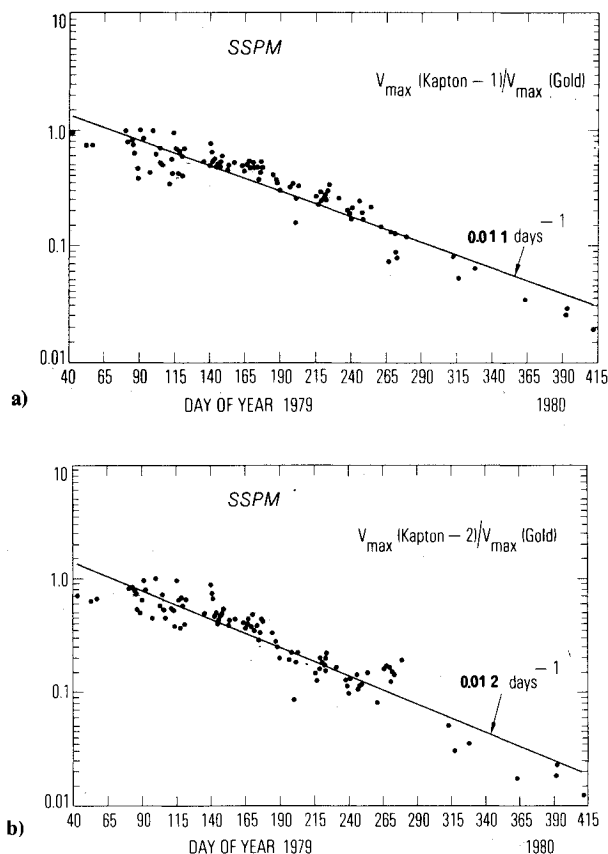


Fig. 9 Ratio of the maximum Kapton voltage in a given 64-s interval to the maximum gold voltage during a 24 h interval: a) SSPM-1 Kapton, b) SSPM-2 Kapton.

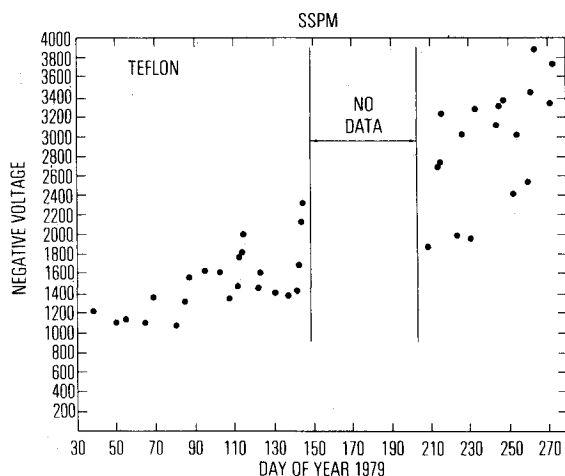


Fig. 10 Teflon bulk voltages vs time.

fects. Increases in the energetic electron fluxes during magnetically disturbed times result in higher charge deposition and enhanced bulk charging in Teflon.¹³ Due to Teflon's very large dark resistivity, the bulk buildup charge is unable to leak off. Every 11 days or so, the P78-2 satellite was maneuvered such that grazing solar incidence on the Teflon sample produced some discharging. Over a period of a few days following these maneuvers, the voltage levels dropped due to the solar uv. The data shown in Fig. 10 were taken a few days before the maneuvers when the samples were in the shadow of the spacecraft. This behavior of the Teflon sample may be a good indication of bulk charge deposition in insulators that can occur in electron circuitry and cables on spacecraft (see Ref. 13 and references therein).

Summary

The SSPM experiment, flown on the P78-2 SCATHA satellite, provided important data. The measurements have been used to validate the mechanism of differential charging as well as to provide quantitative numbers to test computational charging models and laboratory simulations.

For example, the quartz fabric cloth sample was designed to remain at low potentials during charging events because of its high secondary electron yields and the large surface to volume ratio.¹⁴ Early laboratory simulations confirmed this result. However, in space, the quartz fabric charged even higher than Kapton.^{15,16} Our own laboratory results confirmed the space results when realistic flux levels of electrons were used to bombard the sample. The opposite effect was observed from the ungrounded OSR sample, where charging in space only occurred to low levels, contrary to previous laboratory calibrations.

The SSPM potential was also used to infer energetic plasma boundaries. Figure 2 graphically illustrates how the potential from a Kapton sample follows the total electron current above the second crossover energy. From this simple yet effective way of determining charging events, a statistical survey of spacecraft differential charging was completed as a function of local time, altitude, and magnetic conditions.

Information on the electrical properties of insulators was obtained from the SSPM data. Buildup of large potentials (>8 kV) was observed on the samples with Teflon. These bulk voltages were not associated with surface charging and were more or less permanent offsets. During attitude maneuvers of the spacecraft, the Teflon materials were rotated a few degrees into sunlight and the potentials decreased significantly. When the material rotated slowly into shadow, the voltages began to build up again. Whether the charge buildup was correlated with the direct deposit of charge from energetic electrons is yet to be confirmed. Nevertheless, this set of data is a unique method of studying the effects of energetic electron bombardment on insulators.

In the preceding sections, long-term surveys of the two bellyband Kaptons, the gold conductor, and the ungrounded OSRs were discussed. We will summarize briefly the results of the other samples. The fourth sample flown on the SSPM-1 was an indium oxide coated set of OSRs individually grounded to the spacecraft frame. The main purpose of flying the coated OSR sample was to examine the long-term stability of the thin coating. The survey results show no charging greater than 50 V was ever observed.

The grounded sample flown on the SSPM-3 experiment was a gold-flashed coating on aluminized Kapton. No indication of any voltage levels above background was observed in our analysis of the survey data or for the large June 10, 1980 charging event.

Selected charging events were examined when both the bellyband Kaptons and the SSPM-3 samples were charging. During intense events there were times when the Teflon charged to high surface potentials (see Fig. 1). However, the SSPM-3 samples in general and the SSPM-3 Kapton sample in particular did not charge with the same frequency as the bellyband SSPM samples.

Possibly the most important result from the SSPM data analysis was the decrease in the resistance of Kapton when exposed over long periods to the sun.¹⁷ Orders of magnitude changes in the resistivity of Kapton have been observed. These effects appear to be permanent in the space environment but the quantitative analysis must be done under laboratory controlled conditions to verify the observation.

The SSPM experiment continues to produce unique results; unfortunately only a limited number of spacecraft materials and configurations could be flown on the SCATHA satellite. With new advances in material technology, more of these types of experiments are needed.

Acknowledgments

Many people were involved with the SCATHA project over the years and their contributions to the success of the P78-2 satellite program are acknowledged. Special thanks to E. Schnauss and G. Boyd for their efforts on the SSPM project. This research was supported under USAF Contract F04701-82-C-0083.

References

- ¹Whipple, E.C., "Potential of Surface in Space," *Reports on Progress in Physics*, Vol. 44, 1981, p. 1197.
- ²Garrett, H.B., "The Charging of Spacecraft Surfaces," *Reviews of Geophysics and Space Physics*, Vol. 19, 1981, p. 577.
- ³McPherson, D.A. and Schoher, W.R., "Spacecraft Charging at High Altitude: The SCATHA Satellite," *Spacecraft Charging by Magnetospheric Plasmas: AIAA Progress in Astronautics and Aeronautics*, edited by A. Rosen, Vol. 47, AIAA, New York, 1976, p. 89.
- ⁴Stevens, J.R. and Vampola, A.L., Eds., "Description of the Space Test Program P78-2 Spacecraft and Payloads," USAF Space Division, El Segundo, Calif., SAMSO TR-78-24, Oct. 1978.
- ⁵Koons, H.C., Mizera, P.F., Fennell, J.F., and Hall, D.F., "Spacecraft Charging Results from the SCATHA Satellite," *Astronautics and Aeronautics*, Nov. 1980, p. 44.
- ⁶Lehn, W.L., "New Space Materials Development in the United States," *Proceedings of an ESA Symposium on Spacecraft Materials*, ESASP, Vol. 145, 1979, p. 37.
- ⁷Mizera, P.F., Schnauss, E.R., Vandre, R., and Muller, E.G., "Description and Charging Results from the RSPM," *Spacecraft Charging Technology*, 1978, NASA Con. Pub. 2071, AFGL-TR-79-0082, 1979.
- ⁸Mizera, P.F., "Charging Results from the Satellite Surface Potential Monitor," *Journal of Spacecraft and Rockets*, Vol. 18, 1981, p. 506.
- ⁹Leung, M.S., Tueling, M.B., and Schnauss, E.R., "Effects of Secondary Electron Emission on Charging," *Spacecraft Charging Conference*, 1980, AFGL-TR-81-0270, 1981, p. 163.
- ¹⁰Mizera, P.F. and Isenburg, P.A., "Plasma Sheet Boundaries Inferred from Spacecraft Charging Results," *Eos*, Vol. 61, 1980, p. 1091.
- ¹¹Mizera, P.F. and Boyd, G.M., "The Satellite Surface Potential Survey," *Spacecraft Charging Conference III*, 1980, AFGL-TR-81-0270, 1981, p. 461.
- ¹²Reasoner, D.L., Lennartsson, W., and Chappell, C.R., "Relationship Between ATS-6 Spacecraft Charging Occurrences and Warm Plasma Encounters," *Spacecraft Charging by Magnetospheric Plasmas: AIAA Progress in Astronautics and Aeronautics*, edited by A. Rosen, Vol. 47, AIAA, New York, 1976, p. 89.
- ¹³Regan, J.B., Meyeroff, R.E., Gaines, E.E., Nightingale, R.W., Filbert, P.C., and Imhof, W.L., "Space Charging Currents and their Effects on Spacecraft Systems," *Proceedings of the 10th International Symposium on Discharges and Electrical Insulation in Vacuum*, Oct. 1982.
- ¹⁴Belanger, V.J. and Eagles, A.E., "Secondary Emission Conductivity of High Purity Silicon Fabric," *Spacecraft Charging Technology*, 1977, p. 655, AFGL-TR-77-0051, p. 655.
- ¹⁵Mizera, P.F. et al., "First Results of Material Charging in the Space Environment," *Applied Physics Letters*, Vol. 37, 1980, p. 276.
- ¹⁶Mizera, P.F., Leung, S., and Kan, H.K.A., "Laboratory Study of the Charging of Spacecraft Materials," *Journal of Spacecraft and Rockets*, Vol. 18, 1981, p. 510.
- ¹⁷Adamo, R.C. and Nanevich, J.E., "Conductivity Changes in High-Voltage Spacecraft Insulating Materials," *Spacecraft Charging Technology*, 1977, p. 669, AFGL-TR-77-0051.

From the AIAA Progress in Astronautics and Aeronautics Series

SPACECRAFT RADIATIVE TRANSFER AND TEMPERATURE CONTROL—v. 83

Edited by T.E. Horton, The University of Mississippi

Thermophysics denotes a blend of the classical engineering sciences of heat transfer, fluid mechanics, materials, and electromagnetic theory with the microphysical sciences of solid state, physical optics, and atomic and molecular dynamics. This volume is devoted to the science and technology of spacecraft thermal control, and as such it is dominated by the topic of radiative transfer. The thermal performance of a system in space depends upon the radiative interaction between external surfaces and the external environment (space, exhaust plumes, the sun) and upon the management of energy exchange between components within the spacecraft environment. An interesting future complexity in such an exchange is represented by the recent development of the Space Shuttle and its planned use in constructing large structures (extended platforms) in space. Unlike today's enclosed-type spacecraft, these large structures will consist of open-type lattice networks involving large numbers of thermally interacting elements. These new systems will present the thermophysicist with new problems in terms of materials, their thermophysical properties, their radiative surface characteristics, questions of gradual radiative surface changes, etc. However, the greatest challenge may well lie in the area of information processing. The design and optimization of such complex systems will call not only for basic knowledge in thermophysics, but also for the effective and innovative use of computers. The papers in this volume are devoted to the topics that underlie such present and future systems.

552 pp., 6 × 9, illus., \$30.00 Mem., \$45.00 List

TO ORDER WRITE: Publications Order Dept., AIAA, 1633 Broadway, New York, N.Y. 10019